SMN Tudor domain structure and its interaction with the Sm proteins

Philipp Selenko[1,2], Remco Sprangers[1,2], Gunter Stier[1], Dirk Bühler[3], Utz Fischer[3] and Michael Sattler[1]

[1]Structural and Computational Biology, EMBL, Meyerhofstr. 1, D-69012 Heidelberg, Germany. [2]These authors contributed equally to this work. [3]Max-Planck Institut für Biochemie, Am Klopferspitz 18a, D-82152 Martinsried, Germany.

Spinal muscular atrophy (SMA) is a common motor neuron disease that results from mutations in the Survival of Motor Neuron (*SMN*) gene. The SMN protein plays a crucial role in the assembly of spliceosomal uridine-rich small nuclear ribonucleoprotein (U snRNP) complexes *via* binding to the spliceosomal Sm core proteins. SMN contains a central Tudor domain that facilitates the SMN–Sm protein interaction. A SMA-causing point mutation (E134K) within the SMN Tudor domain prevents Sm binding. Here, we have determined the three-dimensional structure of the Tudor domain of human SMN. The structure exhibits a conserved negatively charged surface that is shown to interact with the C-terminal Arg and Gly-rich tails of Sm proteins. The E134K mutation does not disrupt the Tudor structure but affects the charge distribution within this binding site. An intriguing structural similarity between the Tudor domain and the Sm proteins suggests the presence of an additional binding interface that resembles that in hetero-oligomeric complexes of Sm proteins. Our data provide a structural basis for a molecular defect underlying SMA.

Spinal muscular atrophy (SMA) is a motor neuron disease that leads to muscle atrophy due to motor neuron degeneration. SMA is a major genetic cause of early childhood mortality and results from mutations in the Survival of Motor Neuron (*SMN*) gene[1–4]. The 294-residue SMN protein is part of a multimeric complex that includes the spliceosomal Sm core proteins[5–8]. The seven human Sm core proteins are Sm B, D_{1-3}, E, F, and G. Most of the cellular SMN protein is localized in the cytoplasm, where it is crucial for the assembly of spliceosomal uridine-rich small nuclear ribonucleoprotein (U snRNP) complexes[5,6,8,9]. It has been shown that the interaction of SMN with Sm proteins is essential for this process[8,9], during which hetero-oligomeric Sm D_1–D_2, E–F–G and D_3–B complexes are bound to the U snRNAs[10]. SMN contains a central, highly conserved Tudor domain that is required for U snRNP assembly and facilitates Sm protein binding[9]. A SMA-causing point mutation (E134K) within the SMN Tudor domain prevents Sm binding[9]. Several RNA-

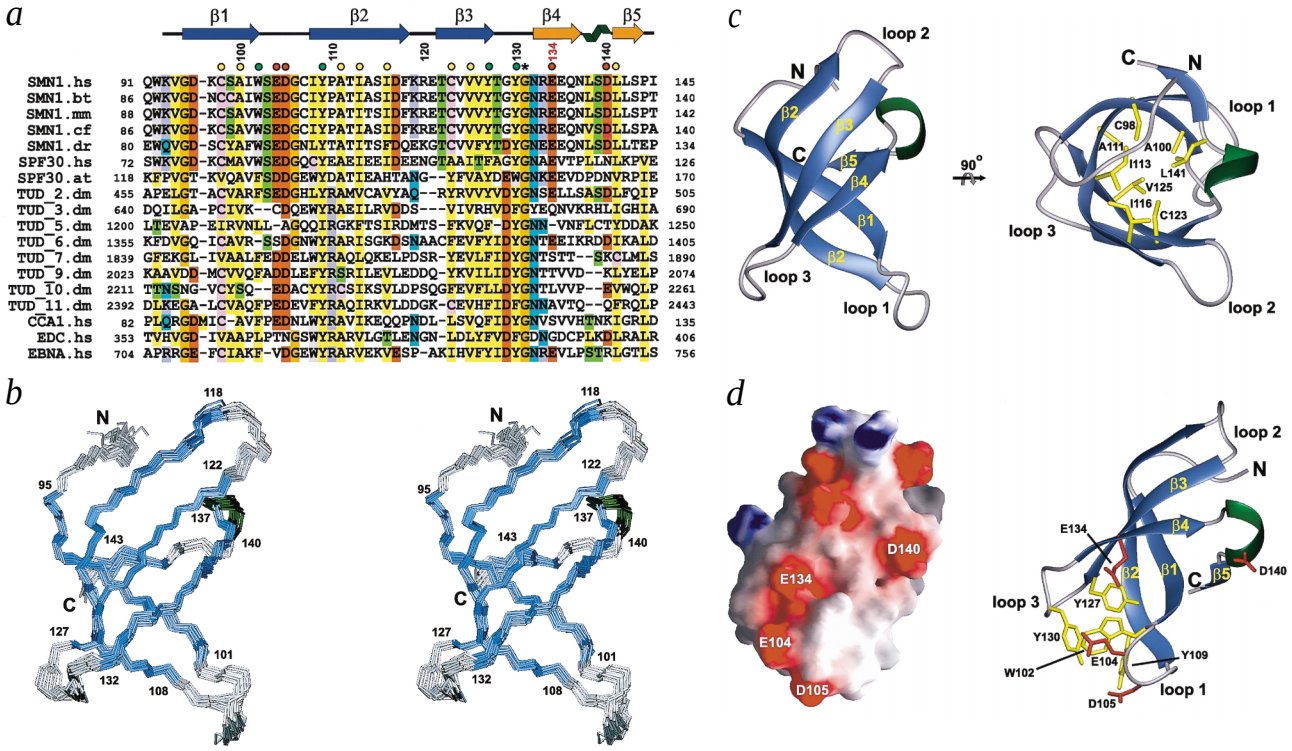

Fig. 1 Structure of the SMN Tudor domain. ***a***, Multiple sequence alignment of Tudor domains. Secondary structure elements defined by the NMR structure of the SMN Tudor domain are shown above the alignment. Conserved hydrophobic, aromatic and negatively charged residues are marked with yellow, green and red circles, respectively. Accession numbers (SWISS-PROT, Genbank or PIR) are: SMN1.hs, Q16637; SMN1.bt, O18870; SMN1.mm, P97801; SMN1.cf, O02771; SMN1.dr, Q9W6S8; SPF30.hs, 5032113; SPF30.at, 7487808; TUD (Tudor protein), A41519; CCA1.hs (colon cancer antigen), 3170162; EDC.hs (epidermal differentiation complex RNA binding protein), 5803195;EBNA.hs (Epstein-Barr virus nuclear coactivator protein), 7657431. ***b***, Stereo view of the backbone atoms (N, Cα, C′) for residues 91–144 of an NMR ensemble of 20 superimposed structures. Secondary structure elements are colored blue. The helical turn connecting β4 and β5 is colored green. The first and last residues of the five β-strands are labeled. ***c***, Left: ribbon representation of the Tudor domain structure closest to the average conformation of the NMR ensemble in the same orientation as in (*b*). Right: rotated view of the Tudor domain structure showing the side chains of hydrophobic core residues in yellow. ***d***, Left: surface representation of the Tudor domain structure. Blue and red colors indicate positive and negative electrostatic surface potential, respectively. Right: ribbon representation shown in the same orientation. Side chains of conserved aromatic and negatively charged residues discussed in the text are indicated.

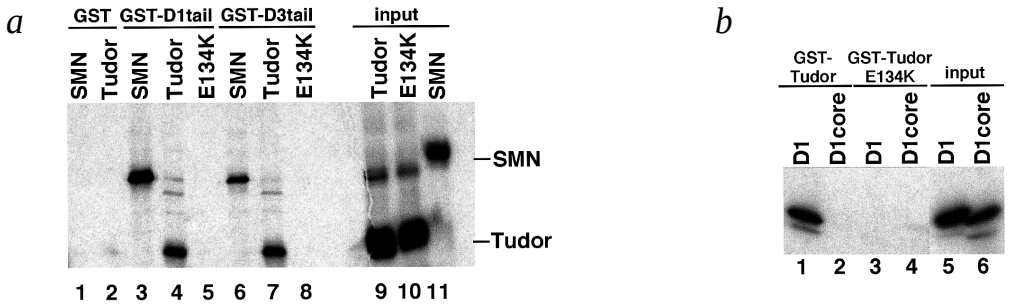

Fig. 2 Sm binding by the SMN Tudor domain. ***a***, Autoradiography exposure of a binding assay using recombinant GST-Sm D_1 and GST-Sm D_3 tails and *in vitro* translated full length SMN (lanes 3 and 6), SMN Tudor domain (lanes 4 and 7) or the E134K mutant Tudor domain (lanes 5 and 8). Input lanes (9–11) show 50% of the translated protein used for binding. As a control, binding of SMN translate (lane 1) and Tudor translate (lane 2) to GST alone are shown. ***b***, Binding of full length Sm D_1 (D1) and the core domain lacking the C-terminal tail (D1core) to recombinant GST-Tudor (lanes 1 and 2) and GST-Tudor harboring the E134K mutation (lanes 3 and 4). Input lanes show 20% of the translated protein (D1, lane 5; D1core, lane 6) used in the binding reaction.

associated proteins contain the Tudor domain, a conserved motif of 50 amino acids[11,12,16]. To gain molecular insight into SMN and its interaction with the spliceosomal Sm proteins, we have solved the three-dimensional structure of the Tudor domain of human SMN.

Structure determination

The solution structure of the Tudor domain of SMN was determined by heteronuclear multidimensional NMR spectroscopy. The recombinant protein used for the structural studies comprised residues 83–173 of human SMN. However, only residues 92–144 (Fig. 1*a*), which correspond to most of exon 3 in the *SMN* gene, adopt a well-defined tertiary structure. The additional N- and C-terminal residues are disordered as indicated by the paucity of nuclear Overhauser effects (NOEs) and small heteronuclear $\{^1H\}$-^{15}N NOE values (data not shown). The protein is monomeric in solution as determined by analytical ultracentrifugation experiments (data not shown). Distance restraints were derived from three-dimensional ^{15}N- and ^{13}C-edited NOE spectra. Orientational restraints were based on residual dipolar couplings measured in a liquid crystalline medium (see Methods). The structure is well-defined by the NMR data that provided more than 29 restraints per residue (Table 1). An ensemble of 20 NMR structures and a ribbon representation of the lowest energy structure are shown in Fig. 1.

Description of the Tudor domain structure

In our three-dimensional structure, the SMN Tudor domain forms a strongly bent antiparallel β-sheet,(Fig. 1*c*). Five strands (β1–5) form a barrel-like fold that is lined at the bottom by the long curved β2 strand and closed by an antiparallel interaction between β1 and Leu 142 in the short β5 strand. Strands β1–4 are connected by short turns, while strand β4 and β5 are linked by a helical turn such that the angle between these two strands is ~90°. The conserved residues Cys 98, Ala 100, Ala 111, Ile 113, Ile 116, Cys 123, Val 125 and Leu 141, stabilize the structure through formation of a hydrophobic core (Fig. 1*c*). Based on the conservation of these structurally important residues (Fig. 1*a*), a similar three-dimensional fold can be expected for other Tudor domains. Furthermore, the conserved aromatic residues Trp 102 (loop 1), Tyr 109 (β2), Tyr 127 (β3) and Tyr 130 (loop 3) form a cluster of hydrophobic side chains between loops 1 and 3 (Fig. 1*d*). Both loops, therefore, adopt a well-defined structure and are not disordered. The conserved Gly 131 appears to be important for the distinct conformation of loop 3. The electrostatic surface representation of the Tudor domain (Fig. 1*d*) exhibits a hydrophobic patch in this region that may be involved in ligand interactions. Next to this hydrophobic surface, several negatively charged amino acids are located in loop 1 (Glu 104, Asp 105), β4 (Glu 134) and the helical turn connecting β4 and β5 (Asp 140). Based on these residues, which are conserved in all SMN homologs and in many other Tudor domain-containing proteins, the structure exhibits an overall negatively charged surface (Fig. 1*a*). These unique structural features suggest that the Tudor domain is more likely to represent a protein interaction domain than to bind to RNA directly[11].

Interaction with Sm proteins

Since SMN binding to Sm proteins is essential for its function[8,9], we further characterized the role of the Tudor domain in this interaction. SMN binds to the Arg and Gly-rich C-terminal tails of the Sm D_1 and D_3 proteins[13]. To investigate whether this interaction could involve the SMN Tudor domain, we performed *in vitro* binding assays. C-terminal tails of Sm D_1 and Sm D_3 were expressed as glutathione-S-transferase (GST) fusion proteins and used in pull-down experiments with *in vitro* translated full length SMN, the Tudor domain or the Tudor domain harboring the E134K mutation. SMN and the Tudor domain bound efficiently to the tails of both Sm D_1 and D_3, whereas the mutant Tudor domain bound to neither (Fig. 2*a*). Conversely, binding to recombinant GST-Tudor domain could be observed for *in vitro* translated Sm D_1 but not for a truncated version lacking the tail (Fig. 2*b*). Again, this interaction was abolished by the E134K mutation. Similar results were obtained using Sm D_3 (data not shown). We conclude, therefore, that the Tudor domain binds to the C-terminal tails of Sm D_1 and D_3.

To localize the binding surface on the Tudor domain structure, we performed NMR titrations with a 23-residue oligopeptide $(GR)_9GGPRR$ derived from the C-terminal tail of Sm D_1. Heteronuclear correlation experiments were recorded on a ^{15}N-labeled Tudor domain to monitor ^1H and ^{15}N chemical shift changes upon addition of the peptide (Fig. 3*a*). The exchange between free and bound protein conformations is fast on the NMR time scale (Fig. 3*a*), which is indicative of a micromolar dissociation constant. The spectral changes show that the Sm D_1 tail binds to a region consisting of loops 1 and 3, including the conserved Gly 131, and neighboring parts of strands β1–4. This surface involves the conserved negatively charged and aromatic

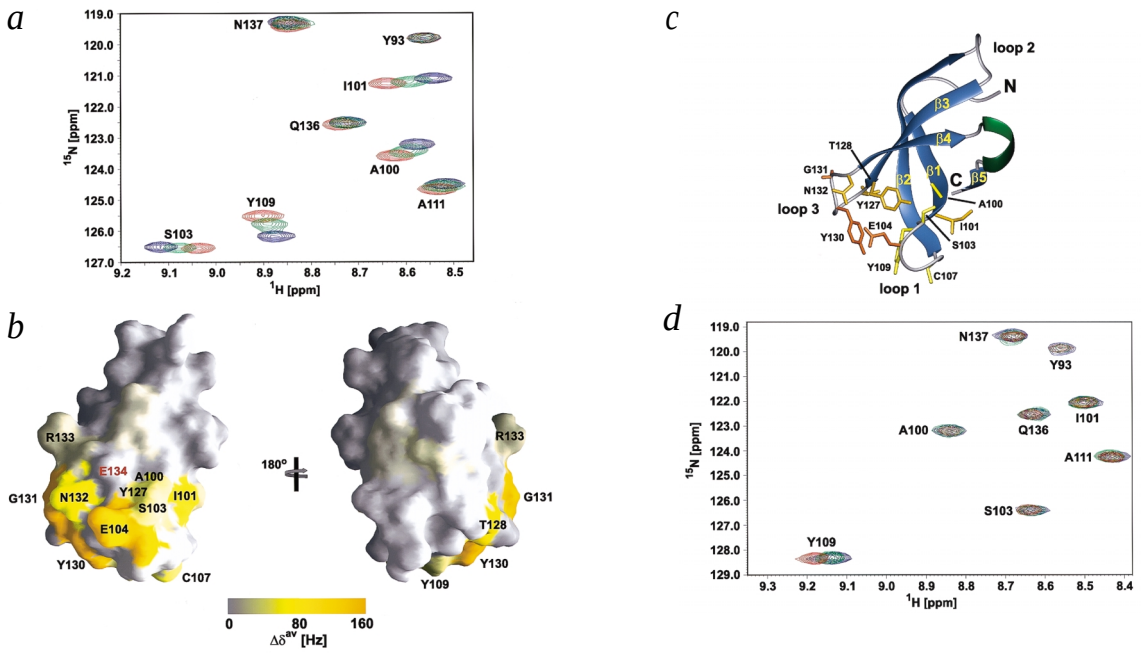

Fig. 3 Mapping the Sm binding site on the Tudor domain structure. ***a***, Results of the NMR titration using a 23-mer peptide comprising the C-terminal tail of the Sm D_1 protein added to a 0.3 mM ^{15}N-labeled SMN Tudor domain sample. ^{1}H,^{15}N correlation spectra corresponding to 0, 0.1 and 0.3 mM peptide are shown in blue, green and red, respectively. ***b***, Residues for which changes are observed during the NMR titration are colored on the surface of the Tudor domain structure. Coloring from gray to orange scales with increasing chemical shift change as indicated ($\Delta\delta^{av} = ((\Delta\delta_{1H})^2 + (\Delta\delta_{15N})^2)^{1/2}$, where $\Delta\delta$ is the chemical shift difference observed at 0 and 0.3 mM peptide). The surface on the left is in the same orientation as in Fig. 1*d*; the surface on the right shows a view from the back side. ***c***, Ribbon representation in the same orientation as in (*b*, left). The side chains of amino acids whose amide groups experience chemical shift changes $\Delta\delta^{av} > 35$ Hz are shown. Color coding from yellow to orange is the same as in (b). ***d***, ^{1}H,^{15}N correlation spectra recorded on a 0.1 mM ^{15}N-labeled sample of the E134K mutant Tudor domain with 0 (blue), 0.1 (green) or 1 mM (red) Sm D_1 tail peptide. Minor chemical shift changes were observed only at 10-fold molar excess of the peptide, confirming that the affinity is severely reduced compared to the wild type Tudor domain.

residues of the Tudor domain (Fig. 3*b*). Thus, a region of the Tudor domain that includes Glu 134 is part of the binding site that recognizes the C-terminal tail of Sm D_1.

To exclude the possibility that the E134K mutation impairs Sm binding by disrupting the three-dimensional structure of the Tudor domain, we prepared recombinant E134K Tudor domain. Comparison of ^{1}H,^{15}N correlation spectra of wild type and mutant proteins revealed chemical shift differences only for residues in close spatial proximity to residue 134. In addition, {^{1}H}-^{15}N NOE experiments (data not shown) confirmed that the E134K mutant Tudor domain remains structured and also excluded the possibility that strand β4 is locally unfolded. In an NMR titration, minor chemical shift changes were observed only at 10-fold molar excess of the $(GR)_9GGPRR$ peptide, confirming that binding to the E134K mutant Tudor domain was severely reduced (Fig. 3*d*). Thus, the E134K mutation changes the local charge distribution at the Sm binding site, which likely affects electrostatic interactions with the positively charged C-terminal Sm tails.

Structural similarity to the Sm protein fold

The three-dimensional structure of the SMN Tudor domain resembles the fold of the Sm core proteins (Fig. 4), even though their amino acid sequences do not share any detectable similarity (Fig. 1*a*). Compared to the Sm fold (Fig. 4)[14], the Tudor domain lacks an N-terminal helix, and strands β3–5 are shorter. Strands β3 and β4 are, therefore, much less curved than the corresponding strands in Sm proteins (Fig. 4*a*). However, the lengths of β3 and β4 are also variable within the Sm protein family[14]. Sm proteins exist as heteromeric complexes in solution[10]. The binding interface in the Sm D_3–B and Sm D_1–D_2 heterodimers consists of an antiparallel β-sheet formed from strand β4 of one monomer and strand β5 of the neighboring Sm protein (Fig. 4*b*)[14]. This interface is further stabilized by hydrophobic and electrostatic interactions.

The intriguing structural similarity between the Tudor domain and the Sm fold suggests that the Tudor domain may form a similar intermolecular β4–β5 interface with a cognate Sm protein, in addition to its interaction with the C-terminal tails of Sm proteins. Despite the fact that we (Fig. 2*b*) and others[13] have not detected such an interaction using *in vitro* binding assays, such a model is supported by the observation that, even though the Sm-like proteins Lsm2, Lsm6 and Lsm7 lack an Arg and Gly-rich tail, they are still able to bind SMN[13]. As a possible explanation, the Tudor–Sm core interaction might be too weak to be detected by *in vitro* binding experiments. Similarly, the β4–β5 interactions between different Sm heterodimers in the snRNP core and subcore complexes[14], for example, Sm B–D_1, Sm D_2–F and Sm G–D_3, are only observed in the presence of Sm site RNA and are not detectable in *in vitro* binding experiments in the absence of RNA[10]. Thus, the formation of a high affinity SMN–Sm complex could require multiple and cooperative interactions, for example, involving Sm core and tail binding to the Tudor domain, and additional regions of the SMN protein[8,9,13].

Conclusion

Our results provide novel structural insights into the interactions between SMN and Sm proteins. These interactions are crit-

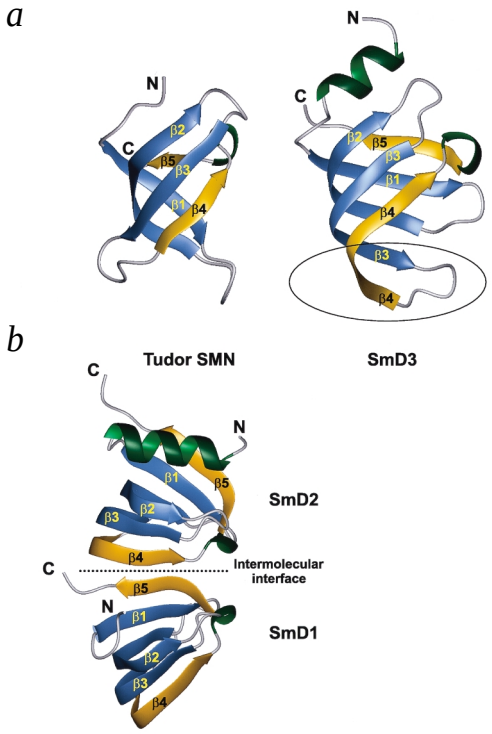

Fig. 4 The Tudor domain resembles a truncated Sm fold. ***a***, Comparison of the SMN Tudor domain structure and the Sm D_3 protein. Both structures share a common fold consisting of a strongly bent five-stranded β-sheet. The backbone r.m.s. deviation for the superposition of 49 residues in Sm D_3 and SMN Tudor is 3 Å. The residue numbers that were superimposed between the Tudor domain and Sm D_3 are: Tudor: 91–101, 105–118, 120–129, 130–137, 140–144; Sm D_3: 11–21, 24–37, 38–47, 57–64, 70-74. The circle indicates the extension of strands β3 and β4 in the Sm D_3 protein that is not observed in the fold of the Tudor domain. ***b***, Crystal structure of the human Sm D_1D_2 heterodimer[14]. The β-strands that form the dimer interface (β5 of Sm D_1 and β4 of Sm D_2) are shown in orange. For Sm D_1, only the core domain (residues 9–72) is shown for clarity. Strands β4 of Sm D_1 and β5 of Sm D_2, also shown in orange, are assumed to form similar interactions with neighboring Sm hetero-oligomers in the heptameric Sm core complex[14].

ical for U snRNP biogenesis, during which the hetero oligomeric Sm D_1–D_2, E–F–G and D_3–B protein complexes are assembled onto U snRNAs in a stepwise and ordered manner[10]. Although an important role in U snRNP assembly has been demonstrated for SMN[5], the mechanistic details remain elusive. Here, we have shown that the Tudor domain but not its E134K mutant interacts with the C-terminal tails of the Sm proteins, and that the binding site maps to a conserved negatively charged region that includes Glu 134 and a hydrophobic cluster of aromatic residues between loops 1 and 3. It should be noted that the Sm D_1 and D_3 tails are post-translationally modified *in vivo* and contain symmetrical dimethylarginines[15]. These modifications could provide a regulatory mechanism for the binding of Sm proteins to SMN. The striking structural similarity between the Tudor and Sm folds suggests that additional interactions between the Tudor domain and an Sm core domain may exist. In contrast to the interaction with the Sm tails, which is presumably mediated by electrostatic attractions, a β4–β5 interaction with a Sm protein core domain could be weaker but may provide additional contacts for specific recognition of an Sm protein. It has been shown that SMN self-associates and is part of a multimeric protein complex with Sm proteins and other SMN interacting proteins[5,6,8]. In such an oligomeric complex, the formation of a specific and high affinity SMN–Sm complex could be established through multiple contact points, involving the Tudor domain and additional regions[8,13] of SMN.

In summary, we present the first structure of the evolutionarily conserved Tudor domain and provide novel insights into the SMN–Sm interactions that are critical for understanding the function of the SMN protein, and thus a molecular basis of SMA. Finally, it is likely that the Tudor domains in other RNA associated proteins function as protein–protein interaction motifs and do not bind to RNA directly.

Methods

Sample preparation. Human SMN cDNA encoding the Tudor domain was inserted into the *NcoI*/*KpnI* sites of a modified pET24d expression vector (Novagen) containing an N-terminal His_6-GST tag followed by a TEV protease cleavage site[17]. The expression clone was confirmed by DNA sequencing. The 94-residue recombinant protein used for the structural studies comprised residues 83–173 of SMN plus four additional residues from the TEV cleavage site. The molecular weight of the protein was confirmed by mass spectrometry. Uniformly ^{15}N-labeled and ^{15}N,^{13}C-labeled proteins were prepared by growing the *Escherichia coli* strain BL21(DE3) overexpressing the SMN Tudor domain in a minimal medium containing $^{15}NH_4Cl$ with or without $^{13}C_6$-glucose and purified as described[17]. Additional purification was achieved with ion exchange chromatography on a Q-sepharose column. NMR samples were

Table 1 Structural statistics for the SMN Tudor domain

		<SA>[1]
Experimental restraints		
	Number of restraints	R.m.s. deviations
Distance restraints (Å)[2]		
Unambiguous	1,402	0.0045 ± 0.0016
Hydrogen bonds	50	0.005 ± 0.002
Dihedral angle restraints (°)[3]	17 ϕ, 6 χ_1	0.09 ± 0.10
Residual dipolar coupling restraints (Hz)		
H–N	44	0.56 ± 0.12
Coordinate precision (Å; residues 92–144)[4]		
N, Cα, C′		0.42 ± 0.09
All heavy atoms		0.88 ± 0.09
Structural quality		
$E_{L\text{-}J.}$[5] (kcal mol^{-1})		-481 ± 6
Ramachandran plot (%)		
Most favored region		80.0 ± 4.1
Additionally allowed region		19.8 ± 4.1

[1]<SA> is the ensemble of the 20 lowest energy structures out of 100 calculated. Root mean square (r.m.s.) deviations for bond lengths, bond angles and improper dihedral angles were 0.00092 ± 0.00004 Å, 0.240 ± 0.003° and 0.119 ± 0.004°, respectively.
[2]No distance restraint was violated by >0.3 Å in any of the final structures.
[3]No dihedral angle restraint was violated by >2.1°.
[4]Coordinate precision is given as the Cartesian coordinate r.m.s. deviation of the 20 lowest energy structures with respect to their mean structure.
[5]$E_{L\text{-}J.}$ is the Lennard-Jones van der Waals energy calculated using the CHARMM PARMALLH6 parameters. $E_{L\text{-}J.}$ was not included in the target function during the structure calculations.

exchanged into 20 mM sodium phosphate buffer (pH 6.3), 30 mM NaCl, 5 mM DTT in 9:1 H_2O:^2H_2O or ^2H_2O at 1.0–1.5 mM concentration. The peptide $(GR)_9GGPRR$, comprising the 23 C-terminal residues of the Sm D_1 protein, was purchased from MWG Biotech (Munich, Germany).

NMR spectroscopy. NMR spectra were recorded at 27 ºC on Bruker DRX 500 and DRX 600 NMR spectrometers. Spectra were processed with NMRPIPE[18] and analyzed using XEASY[19]. Backbone and side chain ^1H, ^{15}N and ^{13}C resonances were assigned using standard triple resonance experiments[20]. Stereospecific assignments of the methyl groups of Val and Leu residues were obtained using a 10% ^{13}C-labeled sample as described[21]. Distance restraints were derived from ^{13}C-edited and ^{15}N-edited 3D NOESY experiments. Dihedral angle restraints for ϕ and χ_1 were obtained from $^3J_{HN-H\alpha}$ and $^3J_{N-C\gamma}$ coupling constants, respectively[22]. Hydrogen bond restraints were derived from slowly exchanging amide protons, identified after exchange of the H_2O buffer to D_2O. ^1H,^{15}N residual dipolar couplings were measured in isotropic and anisotropic (5% 3:1 dimystoyl phosphatidycholine (DMPC) and dihexanoyl phosphatidylcholine (DHPC)) phases[23]. For NMR titrations, chemical shifts were recorded with ^1H,^{15}N heteronuclear single quantum correlation (HSQC) experiments[20] at 600 MHz proton frequency using a 0.3 mM ^{15}N-labeled Tudor domain sample. The concentration of the peptide was increased up to a two-fold molar excess. However, saturation of the binding at equimolar peptide/protein ratio suggests that the Sm tail and the Tudor domain formed a 1:1 complex. For some residues, including Glu 134, chemical shift changes were observed but could not be quantified due to spectral overlap. NMR titrations with the E134K mutant Tudor domain were recorded at 500 MHz proton frequency on a 0.1 mM ^{15}N-labeled protein sample. $\{^1H\}$-^{15}N heteronuclear NOE experiments were recorded and analyzed as described[24].

Structure calculations. The experimentally determined distance and dihedral angle restraints were applied in a mixed torsion and Cartesian angle dynamics simulated annealing protocol with the programs CNS[25] and ARIA[17,26]. Residual dipolar coupling restraints were applied as described[27]. Structural quality was evaluated using PROCHECK[28]. Figures showing three-dimensional structures and molecular surfaces were prepared using MOLMOL[29] and GRASP[30], respectively.

Binding assays. Glutathione-Sepharose (~50 µl; Amersham-Pharmacia) was incubated for 1 h at 4°C with 1 µg of purified recombinant GST-fusion protein. Fragments fused to GST and used for binding assays included the tails of human Sm D_1 and D_3 (residues 68–119 and 72–126, respectively) and the Tudor domain of the wild type and mutated (E134K) human SMN sequence (residues 36–160). For protein binding, 3 µl of ^{35}S-labeled, *in vitro* translated proteins were incubated with the matrix-coupled GST-fusion proteins for 1 h at 4 °C. The resin was subsequently washed extensively with binding buffer (300 mM NaCl, 50 mM Tris-HCl pH 7.4, 5 mM $MgCl_2$). Bound protein was eluted with SDS sample buffer and analyzed by SDS-PAGE followed by autoradiography using Amplify (Amersham). Translates used included full length human SMN, the wild type and mutant (E134K) SMN Tudor domain, Sm D_1, and the Sm D_1 core domain (residues 1–68). The weak bands visible above the Tudor domain translates in Fig. 2*a* represent read-through products that were terminated downstream of the normal stop codon.

Coordinates. Coordinates have been deposited in the Protein Data Bank (accession code 1G5V). Chemical shifts and NOE peak lists have been deposited in the BioMagResBank (accession code 4899).

Acknowledgments
We would like to thank I. Mattaj, M. Bottomley and M. Macias for suggestions and critical reading of the manuscript. We thank J. Rappsilber for stimulating discussions at early stages of the project, and W. Bermel (Bruker, Karlsruhe) for support.

Correspondence should be addressed to M.S. *email: sattler@EMBL-Heidelberg.de*

Received 21 August, 2000; accepted 6 November, 2000.

1. Pearn, J. *Lancet* **1**, 919–922 (1980).
2. Brzustowicz, L.M., *et al. Nature* **344**, 540–541 (1990).
3. Melki, J. *et al. Nature* **344**, 767–768 (1990).
4. Lefebvre, S. *et al. Cell* **80**, 155–165 (1995).
5. Liu, Q., Fischer, U., Wang, F. & Dreyfuss, G. *Cell* **90**, 1013–1021 (1997).
6. Fischer, U., Liu, Q. & Dreyfuss, G. *Cell* **90**, 1023–1029 (1997).
7. Pellizzoni, L., Kataoka, N., Charroux, B. & Dreyfuss, G. *Cell* **95**, 615–624 (1998).
8. Pellizzoni, L., Charroux, B. & Dreyfuss, G. *Proc. Natl. Acad. Sci. USA* **96**, 11167–11172 (1999).
9. Bühler, D., Raker, V., Lührmann, R. & Fischer, U. *Hum. Mol. Genet.* **8**, 2351–2357 (1999).
10. Raker, V.A., Hartmuth, K., Kastner, B. & Lührmann, R. *Mol. Cell. Biol.* **19**, 6554–6565 (1999).
11. Ponting, C.P. *Trends Biochem. Sci.* **22**, 51–52 (1997).
12. Talbot, K., Miguel-Aliaga, I., Mohaghegh, P., Ponting, C.P. & Davies, K.E. *Hum. Mol. Genet.* **7**, 2149–2156 (1998).
13. Friesen, W.J. & Dreyfuss, G. *J. Biol. Chem.* **275**, 26370–26375 (2000).
14. Kambach, C. *et al. Cell* **96**, 375–387 (1999).
15. Brahms, H. *et al. J. Biol. Chem.* **275**, 17122–17129 (2000).
16. Neubauer, G. *et al. Nature Genet.* **20**, 46–50 (1998).
17. Liu, Z., *et al. Structure* **7**, 1557–1566 (1999).
18. Delaglio, F. *et al. J. Biomol. NMR* **6**, 277–293 (1995).
19. Bartels, C., Xia, T.-H., Billeter, M., Güntert, P. & Wüthrich, K. *J. Biomol. NMR* **5**, 1–10 (1995).
20. Sattler, M., Schleucher, J. & Griesinger, C. *Prog. NMR Spectrosc.* **34**, 93–158 (1999).
21. Neri, D., Szyperski, T., Otting, G., Senn, H. & Wüthrich, K. *Biochemistry* **28**, 7510–7516 (1989).
22. Clore, G.M. & Gronenborn, A.M. *Tibtech* **16**, 22–34 (1998).
23. Ottiger, M., Delaglio, F. & Bax, A. *J. Magn. Reson.* **131**, 373–378 (1998).
24. Farrow, N.A. *et al. Biochemistry* **33**, 5984–6003 (1994).
25. Brünger, A.T. *et al. Acta Crystallogr. D* **54**, 905–921 (1998).
26. Nilges, M. & O'Donoghue, S.I. *Prog. NMR Spectrosc.* **32**, 107–139 (1998).
27. Tjandra, N., Omichinski, J.G., Gronenborn, A.M., Clore, G.M. & Bax, A. *Nature Struct. Biol.* **4**, 732–739 (1997).
28. Laskowski, R.A., Rullmannn, J.A., MacArthur, M.W., Kaptein, R. & Thornton, J.M. *J. Biomol. NMR* **8**, 477–486 (1996).
29. Koradi, R., Billeter, M. & Wüthrich, K. *J. Mol. Graph.* **14**, 51–55 (1996).
30. Nicholls, A., Sharp, K.A. & Honig, B. *Proteins* **11**, 282 (1991).